RESEARCH ARTICLE
doi: 10.2306/scienceasia1513-1874.2023.067

ScienceAsia 49 (2023): **661–669**

Genomic analysis and physicochemical screening of ikarugamycin, fumaquinone, and a new compound, pudicin from *Streptomyces* sp. 3MP-14

Nattaporn Klykleung[a,†], **Hirotaka Matsuo**[b,c,†], **Masato Iwatsuki**[c], **Yōko Takahashi**[c], **Satoshi Ōmura**[c], **Masahiro Yuki**[d], **Takuji Kudo**[d], **Moriya Ohkuma**[d], **Rataya Luechapudiporn**[e], **Somboon Tanasupawat**[a,*], **Takuji Nakashima**[c,f]

[a] Department of Biochemistry and Microbiology, Faculty of Pharmaceutical Sciences, Chulalongkorn University, Bangkok 10330 Thailand
[b] Research Center for Medicinal Plant Resources, National Institutes of Biomedical Innovation, Health and Nutrition, 1-2 Hachimandai, Tsukuba 305-0843 Japan
[c] Ōmura Satoshi Memorial Institute, Kitasato University, 5-9-1 Shirokane, Minato-ku, Tokyo 108-8641 Japan
[d] Japan Collection of Microorganisms, RIKEN BioResource Research Center, 3-1-1 Koyadai, Tsukuba, Ibaraki 305-0074 Japan
[e] Department of Pharmacology and Physiology, Faculty of Pharmaceutical Sciences, Chulalongkorn University, Bangkok 10330 Thailand
[f] Research Organization for Nano and Life Innovation, Waseda University, 513 Waseda, Tsurumaki-cho, Shin-juku-ku, Tokyo 162-0041 Japan

*Corresponding author, e-mail: Somboon.T@chula.ac.th
† These authors contributed equally to this work.

Received 16 Jan 2023, Accepted 4 Jun 2023
Available online 12 Aug 2023

ABSTRACT: An endophytic actinomycete, strain 3MP-14 isolated from the root of *Mimosa pudica* belonged to the genus *Streptomyces* and was closely related to *Streptomyces mimosae* JCM 33328^T (100%) based on 16S rRNA gene sequences. The strain had genome sizes of 7.2 Mb with genomic G+C contents of 73.4 mol%. The average nucleotide identity (ANI) and digital DNA-DNA hybridization (dDDH) of strain 3MP-14 were 100% when compared with *S. mimosae* JCM 33328^T. Based on the polyphasic approach, dDDH, and ANI, strain 3MP-14 was identified as *Streptomyces mimosae*. Twenty-four putative secondary metabolite biosynthetic gene clusters (BGCs) were identified from the draft genome analysis of strain 3MP-14. In the course of chemical investigation for the products of the strain, a physicochemical (PC) screening was conducted, and a new compound, designated as pudicin, and two known antimicrobials, ikarugamycin and fumaquinone, were identified. The structure elucidation of pudicin revealed a unique structurally new compound with *N*-acetylcysteine moiety using one-dimensional and two-dimensional nuclear magnetic resonance (1D and 2D NMR spectroscopy) and Electrospray Ionization Mass Spectrometry (ESI-MS). Pudicin showed slight antioxidative activity based on 2,2-diphenyl-1-picrylhydrazyl (DPPH) radical scavenging method with the IC_{50} value of 394.89 ± 3.88 μg/ml.

KEYWORDS: actinomycetes, physicochemical screening, pudicin, *Mimosa pudica*, *Streptomyces*, secondary metabolite

INTRODUCTION

The genus *Streptomyces* is aerobic, Gram-positive filamentous bacteria that form spore chains on the extensively branched substrate and aerial mycelia. *Streptomyces* species have LL-diaminopimelic acid and no diagnostic sugar in whole-cell hydrolysates. They are widely distributed in various habitats, including terrestrial, hot springs, marine, desert, and plants [1]. Over 50 percent of microbial compounds were produced from actinomycetes, especially the genus *Streptomyces* which was the largest bioactive producer among the others [2]. Endophytic actinomycetes which resided in the tissues of healthy host plants as endosymbionts are the potential resources of new species and new secondary metabolites for developing new drug discovery with many drugs and analogs successfully used in clinical practice [3, 4]. Special pressure and selective environment have led to evolution of endophytes to produce new enzymes for adapting to their hosts, enabling the biosynthesis of new secondary metabolites [5, 6]. In addition, many traditional medicinal plants have widely local ethnobotanical use in alternative medicine in Thailand. Thus, medicinal plants are promising as isolation sources for discovering new endophytic actinomycetes and novel bioactive compounds in this study.

A program designed to discover new endophytic actinomycetes and their bioactive secondary metabolites was investigated. The search for new secondary compounds was optimized by physicochemical (PC) screening [2, 7] based on the spectrum obtained from liquid chromatography with tandem mass spectroscopy (LC/MS/MS) data and compared with the

natural product databases in the Dictionary of Natural Products (http://dnp.chemnetbase.com). Therefore, in this study we investigated the taxonomic position of strain 3MP-14 isolated from the root of *M. pudica* (*Fabaceae*) based on polyphasic approaches and the mass and ultraviolet (UV) spectra of the potential antimicrobials identified. Additionally, the antioxidative activity of the new compound was determined using 2,2-diphenyl-1-picrylhydrazyl (DPPH) radical scavenging method with the half maximal inhibitory concentration (IC_{50}) value.

MATERIALS AND METHODS

Isolation and identification of strain 3MP-14

The root of *M. pudica* (*Fabaceae*) was collected from Kanchanaburi Province, Thailand (14°31′12″ N 98°49′15″ E), and strain 3MP-14 was isolated as previously described [8]. After incubation on International *Streptomyces* Project (ISP) 4 medium at 30 °C for 30 days, morphological characteristics were observed by a scanning electron microscope (model JSM-5600, JEOL, Tokyo, Japan). Cultural characteristics were investigated on ISP media [9]: ISP 2, ISP 3, ISP 4, ISP 5, ISP 6, ISP 7, and nutrient agar plates. The aerial and substrate mycelia and soluble pigments were determined using the National Bureau of Standards (NBS)/Inter-Society Color Council (ISCC) color chart [10]. Carbon utilization was performed as described by Shirling and Gottlieb [9]. Biochemical characteristics, temperatures, pH, and NaCl concentrations for growth were observed as described by Klykleung et al [8]. API ZYM system (bioMérieux, Marcy-l'Étoile, France) was used to determine enzymatic activities. Whole-cell sugars and diaminopimelic acid were evaluated as reported by Staneck and Roberts [11]. Phospholipids were analyzed following the method of Minnikin et al [12]. Menaquinones were analyzed by the method of Collin et al [13]. Cellular fatty acids were analyzed as reported by Sasser [14].

Genomic DNA was isolated and purified as reported previously [15]. The 16S rRNA gene was amplified and sequenced by Macrogen (Seoul, Korea) using universal primers as previously described by Lane [16]. The Basic Local Alignment Search Tool (BLAST) analysis was assessed using the EzBioCloud web-based tool. The neighbor-joining phylogenetic tree was reconstructed using Molecular Evolutionary Genetics Analysis (MEGA) 11 [17]. Whole-genome sequencing was carried out by an Illumina Miseq platform (Illumina) using 2×250 bp paired-end reads. Assembly of the reads to contigs was accomplished by using St. Petersburg genome assembler (SPAdes) 3.12 [18]. The draft assemblies have been submitted to GenBank and are publicly available. Average nucleotide identity (ANI) values were calculated with pairwise genome alignment of the draft genome sequences of related type strains by JSpeciesWS web service [19, 20]. Calculation of the digital DNA-DNA hybridization (dDDH) values was performed by the Genome-to-Genome Distance Calculator (GGDC 2.1) using the BLAST+ method [21]. The G+C content was determined according to the genomic DNA sequences. Results were evaluated by the recommended formula 2 (identities/HSP length), which is useful when dealing with the draft genomes.

Genomic analysis of strain 3MP-14

The draft genome of strain 3MP-14 was annotated by the National Center for Biotechnology Information (NCBI) Prokaryotic Genome Annotation Pipeline [22], Glimmer v3.02 [23], and Rapid Annotation using Subsystem Technology [24]. Identification of potential secondary metabolite biosynthetic gene clusters was achieved using antibiotics and Secondary metabolite Analysis Shell (antiSMASH) v6.0 [25] and confirmed with manual BLAST alignment.

Preliminary screening for antimicrobial activity

The strain was cultivated in seed medium 301 [26] at 30 °C for 5 days (on a 200 rpm shaker) and in a production medium (ISP 2) for 7 days. The ethanol crude extract was screened for its antimicrobial activity against *Staphylococcus aureus* ATCC 25923, *Kocuria rhizophila* ATCC 9341, *Bacillus subtilis* ATCC 6633, *Escherichia coli* ATCC 25922, *Pseudomonas aeruginosa* ATCC 27853, and *Candida albicans* ATCC 10231 using agar well diffusion method [26, 27]. The plates were then incubated at 37 °C for 24 h, except for the *C. albicans* ATCC 10231, which was incubated at 30 °C.

Fermentation and purification of a new compound, pudicin

Briefly, strain 3MP-14 was cultivated in 200 ml of the seed medium (shaking at 200 rpm) at 30 °C for 4 days. The inoculum was transferred into a 30-liter jar fermenter containing 20 l of the production medium (2.5% soluble starch, 1.0% dry yeast, 1.0% defatted wheat germ, 0.5% glycerol, 0.3% meat extract, and 0.3% $CaCO_3$; adjusted to pH 7.0 before sterilization) with aeration 10 l/min and agitation of 250 rpm at 30 °C for 7 days. Purification of a new compound, pudicin, was subsequently guided by its physicochemical properties such as MS and UV spectra, using liquid chromatography/ultraviolet (LC/UV) and liquid chromatography/mass spectrometry (LC/MS) equipment. The purification procedure of pudicin is summarized in Fig. 1. Twenty liters of culture broth were centrifuged; the supernatant was passed through a column of Diaion HP-20 (100 i.d. × 250 mm, Mitsubishi Chemical Co., Tokyo, Japan). After washing with water, the fraction containing pudicin was eluted with methanol (MeOH) and concentrated *in vacuo*. This fraction was dissolved in H_2O, and 3 volumes of ethyl acetate (EtOAc) were added. The EtOAc layer was collected

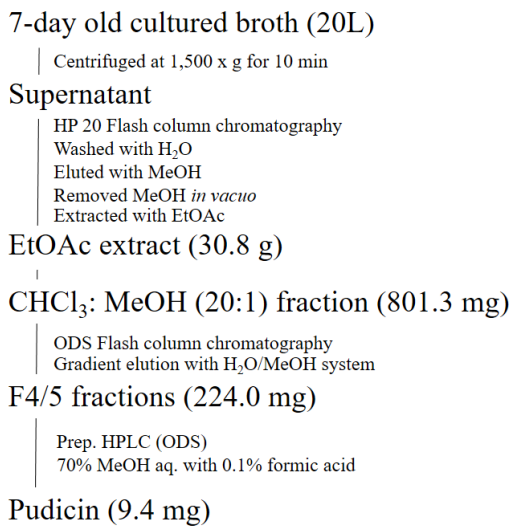

Fig. 1 Purification scheme for pudicin.

and concentrated *in vacuo*, yielding 30.8 g of material. This material was separated into 4 fractions by silica gel column chromatography (60 i.d. × 200 mm, Fuji Silysia Chemical Co., Ltd., Aichi, Japan) with hexane and EtOAc solvent system (hexane:EtOAc = 8:2, 6:4, stepwise separation), followed by chloroform ($CHCl_3$) and MeOH solvent system ($CHCl_3$:MeOH = 20:1, 8:2, stepwise separation). The eluted fraction ($CHCl_3$:MeOH = 20:1) containing pudicin was concentrated to yield 801.3 mg. The material was applied on an ODS column (25 i.d. × 100 mm, Fuji Silysia Chemical Co., Ltd.) and eluting system (0–100% gradient system with MeOH aq. in 30 min and followed by 100% MeOH for 20 min, flow rate 20 ml/min) to give 5 fractions every 10 min. The fourth fraction (224.0 mg) containing pudicin was subjected to semi-preparative High Performance Liquid Chromatography (HPLC) (10 i.d. × 250 mm; YMC-Actus Triart PFP, YMC Co., Ltd., Kyoto, Japan) using a 70% MeOH aq. (0.1% formic acid) isocratic solvent system to obtain pudicin (17.7 mg). The final purification was performed by preparative HPLC (10 i.d. × 250 mm; YMC-Actus C18, YMC Co., Ltd.) using 80% MeOH aq. (0.1% formic acid) isocratic solvent system to obtain pudicin (9.4 mg).

General experimental procedures for chemical analyses

^{1}H-NMR at 400 MHz and ^{13}C-NMR at 100 MHz at 600 MHz (AVANCE III HD600; Bruker, Kanagawa, Japan) were performed. Chemical shifts are expressed in parts per million and referenced to residual CD_3OD (3.31 ppm) and $CDCl_3$ (7.26 ppm) in the ^{1}H-NMR spectra and CD_3OD (49.0 ppm) and $CDCl_3$ (77.0 ppm) in the ^{13}C-NMR spectra. LC/electrospray ionization (ESI)/MS spectra were measured using an MS system (TripleTOF 5600$^+$ System; AB Sciex, Framingham, MA, USA) coupled to a HPLC system (ExionLC AC; AB Sciex). Infrared (IR) spectra were recorded using an IR spectrometer (FT-710; Horiba Ltd., Kyoto, Japan). UV spectra were obtained using a spectrophotometer (U-2810; Hitachi High-Tech Science Co, Tokyo, Japan). Optical rotation was measured on a polarimeter (DIP-1000; JASCO Co, Tokyo, Japan). All solvents were purchased from Kanto Chemical Co., Inc., Tokyo, Japan.

In vitro antioxidant activity of pudicin using DPPH radical scavenging assay

The DPPH radical scavenging activity was determined following the procedure of Chansriniyom et al [28]. The 200 µl of pudicin (0.05–1.0 mg/ml) in EtOH was added to 0.2 ml of a 0.002% DPPH solution in 96-well microplates (NUNC, Gillingham, UK). The reaction was incubated for 30 min in the dark at room temperature. The absorbance was measured using a Corona Grating Microplate Reader SH-9000 (Corona Electric, Ibaraki, Japan) at 517 nm. Ascorbic acid was used as a positive control. The percentage of DPPH radical scavenging activity was calculated as follows:

$$\text{DPPH radical scavenging activity (\%)} = \frac{(A_c - A_s)}{A_c} \times 100$$

where A_c and A_s mean the absorbance of control and sample, respectively. The experiment was conducted in triplicate. The percentage of inhibition at each concentration was measured, and IC_{50} was calculated.

Ferric reducing antioxidant power (FRAP) assay

The ferric (Fe^{+3}) reduction of pudicin (at the final concentration of 1 mg/ml) was carried out according to the method of Wong et al [29]. The ferric-reducing ability of plasma (FRAP) reagent was prepared by mixing 300 mM acetate buffer (pH 3.6), 10 mM 2,4,6-tripyridyl-s-triazine (TPTZ), and 20 mM $FeCl_3 \cdot 6\,H_2O$ in a ratio of 10:1:1 at 37 °C. The 20 µl of pudicin or ascorbic acid (positive control) was added to 96-well microplates (NUNC, Sigma Aldrich, UK), followed by 280 µl of FRAP reagent. The reaction mixtures were incubated in the dark at room temperature for 15 min, and then the absorbances were measured at 593 nm. The Fe^{+3} reduction was calculated as follows: The reduction of Fe^{+3} is expressed in µM of ascorbic acid equivalents by calculating from the calibration curve. FRAP calibration graphs were constructed by plotting absorbances (minus reagent blanks) versus each concentration of the standard in the assay system (µM).

Statistical analysis

Data were calculated as means ± standard deviation (SD). Significant differences were tested by one-way

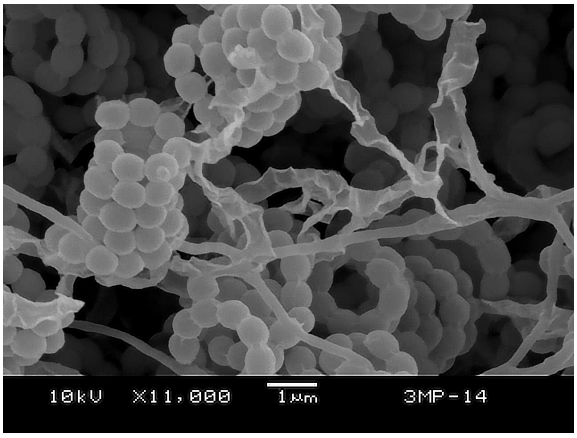

Fig. 2 Scanning electron micrograph of strain 3MP-14 grown on ISP 4 agar medium at 30 °C for 30 days. Bar, 1 μm.

ANOVA for the separation of means (SPSS 15.0 for windows).

RESULTS AND DISCUSSION

Isolation and identification of strain 3MP-14

Strain 3MP-14 (=JCM 33207= TISTR 2647) grew well on ISP 4 and nutrient agar and moderately on ISP 2, ISP 3, and nutrient agar, whereas it grew poorly on ISP 5, ISP 6, and ISP 7 media (Table S1). White aerial masses were formed on ISP 3 and ISP 4 media. The soluble pigment was not produced on the tested media. Spiral spore chains with 4 to 6 turns, circular to elliptical shape (0.5–0.7 × 0.6–0.8 μm in size), and smooth on-surface spores were formed on ISP 4 medium (Fig. 2). The whole-cell hydrolysates of the strain contained LL-diaminopimelic acid, glucose, and ribose. The menaquinones were MK-9 (H_8), MK-10 (H_6), and MK-10 (H_8). The predominant fatty acid was *iso*-$C_{16:0}$ (50.8%) (Table S3). The phospholipids were phosphatidylethanolamine (PE), phosphatidylinositol (PI), diphosphatidylglycerol (DPG), phosphatidylglycerol (PG), unidentified phosphoglycolipid (PGL), and unidentified phospholipid (PL) (Fig. S1). Growth of this strain occurred at 20–37 °C (optimum 30 °C), pH 6.0–11.0 (optimum pH 7.0–9.0), and 0–3% NaCl (w/v). The 16S rRNA gene sequence of strain 3MP-14 revealed that it was closely related to *S. mimosae* 3MP-10^T (100%), *S. zhaozhouensis* DSM 42101^T (98.76%), *S. sedi* JCM 16909^T (98.45%), and *S. triticirhizae* DSM 107172^T (98.35%). The phylogenetic tree showed it was on the same node and shared the cluster with strain 3MP-10^T (Fig. S2). Strain 3MP-14 showed the difference in utilization of *myo*-inositol and enzyme activities of cystine arylamidase, α-chymotrypsin, and α-fucosidase from *S. triticirhizae* DSM 107172^T [30], *S. mimosae* 3MP-10^T, *S. zhaozhouensis* DSM 42101^T, and *S. sedi* JCM 16909^T as shown in Table 1 and Table S2.

The draft genome sequence of strain 3MP-14 was 7,197,316 bp in size with the average *in silico* DNA G+C content of 73.4 mol% (Table 2). The dDDH value between the genomes of strain 3MP-14 and 3MP-10^T was 100% (C.I. model 100–100%), while the dDDH values between the genomes of these strains and related species, including *S. triticirhizae* DSM 107172^T (RFFJ00000000), *S. zhaozhouensis* DSM 42101^T (OCNE00000000), and *S. sedi* JCM 16909^T (VDGT00000000) were 55.7% (C.I. model 52.9–58.4%), 29.9% (C.I. model 27.5–32.4%) and 29.6% (C.I. model 27.2–32.1%), respectively (Table S4). These values were significantly lower than the threshold value of 70% commonly used to delineate separated species status [31]. The ANIb and ANIm values of the draft genomes between strain 3MP-14 and *S. mimosae* 3MP-10^T were 100%. ANIb values between this strain and related species, *S. triticirhizae* DSM 107172^T, *S. zhaozhouensis* DSM 42101^T, and *S. sedi* JCM 16909^T were 94.49, 84.88 and 84.74%, respectively. ANIm values between this strain and related species, *S. zhaozhouensis* DSM 42101^T and *S. sedi* JCM 16909^T were 94.62, 88.01 and 87.92%, respectively (Table S4). Both dDDH and ANI values of strain 3MP-14 and *S. mimosae* 3MP-10^T were 100% which indicated it was identified as *Streptomyces mimosae* [8, 19].

The GenBank/EMBL/DDBJ accession number for 16S rRNA gene sequences of strain 3MP-14 is LC379255. The Whole Genome Shotgun project of strain 3MP-14 has been deposited at DDBJ/ENA/GenBank, and the accession number is VDLZ00000000.

Genomic analysis of strain 3MP-14

A total of 6,077 coding genes from the draft genome of strain 3MP-14 were predicted by RAST, of which 34% were hypothetical. Genome sequence analysis of strain 3MP-14 revealed the presence of at least 24 candidate BGCs. Twenty-four putative secondary metabolite BGCs, predicted in the draft genome of strain 3MP-14, comprised 10 different types of BGCs, including non-ribosomal peptide synthetase (NRPS), polyketide synthetase (PKS), thiopeptide, lanthipeptide, terpenes, butyrolactone, bacteriocin, siderophores, ectoine, and tRNA-dependent cyclodipeptide synthases. The BGCs potentially involved in the biosynthesis of secondary metabolites are presented in Table 3.

The investigation of BGCs in strain 3MP-14 with the known gene clusters was equal to 100% and over 50%. This finding might possibly indicate an ability for the biosynthesis of naringenin, geosmin, ectoine, polyketomycin, and desferrioxamine. As an instance of below 20% gene similarity to the known BGCs, strain 3MP-14 showed hits with different metabolites: 3% similarity to murayaquinone and lactonamycin; 7% similarity to marinophenazine; 8% similarity to azicemicin, cahuitamycins, and chlortetracycline; 12%

Table 1 Differential characteristics of strain 3MP-14 and related type strains. Strains: 1, 3MP-14; 2, *S. mimosae* 3MP-10^T; 3, *S. triticirhizae* DSM 107172^T; 4. *S. zhaozhouensis* DSM 42101^T; and 5, *S. sedi* JCM 16909^T. +, positive; w, weakly positive; −, negative. Data are from this study, except strain DSM 107172^T [30].

Characteristic	1	2	3	4	5
Soluble pigment on ISP 3	None	None	None	None	Dark green
NaCl tolerance (%, w/v)	0–3	0–3	0–6	0–7	0–5
pH range for growth	6–11	6–11	4–6	6–10	7–8
Growth temperature (°C)	20–37	20–37	15–45	15–37	15–37
Nitrate reduction	−	−	−	+	−
Starch hydrolysis	+	+	+	+	−
Gelatin liquefaction	−	−	+	+	−
Utilization of					
L-Arabinose	+	+	−	−	−
D-Fructose	+	+	−	−	+
D-Galactose	+	+	−	+	−
myo-Inositol	+	w	−	−	−
Lactose	+	+	−	+	−
D-Maltose	w	w	−	+	+
D-Mannitol	+	+	−	+	−
D-Mannose	+	+	+	−	−
L-Rhamnose	+	+	−	−	−
D-Ribose	+	+	+	−	−

Table 2 Genome features of strain 3MP-14 and related type strains.

Feature	3MP-14	*S. mimosae* 3MP-10^T	[a] *S. triticirhizae* DSM 107172^T	[a] *S. zhaozhouensis* DSM 42101^T	*S. sedi* JCM 16909^T
Accession no.	VDLZ00000000	VDLY00000000	RFFJ00000000	OCNE00000000	VDGT00000000
Genome size (bp)	7,197,316	7,198,341	6,563,286	6,532,426	6,603,797
Genome coverage	300X	300X	252X	143X	300X
Number of contig	38	45	428	64	51
Total gene	6,145	6,149	6,029	5,625	5,598
The no. of CDS	6,077	6,081	5,696	5,559	5,534
DNA GC content (%)	73.4	73.4	73.3	73.4	72.9

[a] Data from GenBank.

similarity to ikarugamycin; 13% similarity to maklamicin; and 14% similarity to versipelostatin. Nevertheless, several key genes in the metabolic pathways were absent; it is ambiguous to investigate the eventual function of each biosynthetic gene cluster in synthesizing each secondary metabolite. The BGCs with a low percentage of similarity to known clusters may not represent functional gene clusters, or they may be complemented by genes in other regions. Several genes exhibited minimal similarity to known BGCs; some may even be part of other gene clusters due to their composition of one or two genes. Further investigation is required to explain the role of these pathways.

PC screening for secondary metabolites of strain 3MP-14

The culture broth of strain 3MP-14 showed antibacterial activity against *S. aureus* ATCC 25923, *K. rhizophila* ATCC 9341, and *B. subtilis* ATCC 6633. Therefore, it is suggested that antimicrobial agents were included in the culture broth of strain 3MP-14. The culture broth of strain 3MP-14 was added to equal volumes of ethanol and analyzed by LC/UV and LC/MS. The Mass and UV spectra of each peak were compared with those of known compounds using existing databases such as the Dictionary of Natural Products (http://dnp.chemnetbase.com) as well as in-house databases. One new polycyclic aromatic compound, named pudicin, together with two known compounds, fumaquinone and ikarugamycin were found (Fig. S3). Fumaquinone (m/z 303.1223 $[M+H]^+$ calculated value for $C_{17}H_{19}O_5$ 303.1227) exhibited maximal UV absorbance at 220, 265, 304, and 428 nm. Ikarugamycin (m/z 479.2912 calculated value for $C_{29}H_{39}O_4N_2$ 479.2910) exhibited maximal UV at 224 and 326 nm. Ikarugamycin and fumaquinone are known for their wide range of antimicrobials [31, 32].

Structure elucidation of a new compound, pudicin

Pudicin was isolated as a pale yellow amorphous solid; $[\alpha]_D^{30}$ −114.1° ($c = 0.1$, MeOH), IR (KBr) ν_{max}

Table 3 Potential BGCs in the genome of strain 3MP-14.

No.	Type	Length (bp)	Similar BGC (gene no.)	Similarity (%)[a]
1	T1PKS	36,422	Maklamicin	13
2	hgIE-KS	46,138	–	–
3	T2PKS, T1PKS, PKS-like	72,486	Polyketomycin	83
4	Terpene	21,218	Chlortetracycline	8
5	Bacteriocin	10,849	–	–
6	Siderophore, T1PKS	90,234	Tirandamycin	33
7	LAP, thiopeptide	24,706	–	–
8	Terpene	21,841	Hopene	30
9	T3PKS	29,740	Naringenin	100
10	CDPS	20,822	Marinophenazine	7
11	Terpene	22,406	Geosmin	100
12	Lanthipeptide	37,024	Cahuitamycins	8
13	Butyrolactone	9,942	Murayaquinone	3
14	Butyrolactone, PKS-like	31,646	Lactonamycin	3
15	NRPS, Butyrolactone	60,372	Azicemicin	8
16	T1PKS, NRPS	49,372	Ikarugamycin	12
17	Terpene	19,277	Isorenieratene	42
18	Terpene	21,221	Isorenieratene	25
19	T1PKS	33,735	Meoabyssomicin/Abyssomicin	25
20	T3PKS, other	43,440	Furaquinocin	34
21	Siderophore	8,791	Desferrioxamine	50
22	Ectoine	10,396	Ectoine	100
23	T1PKS	12,066	Laidlomycin	28
24	T1PKS	10,531	Versipelostatin	14

[a] The percentage of genes in reference BGC showing similarity to the BGC, which is calculated by antiSMASH.

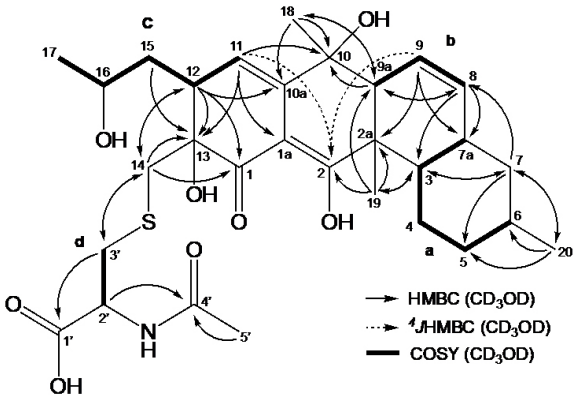

Fig. 3 ^{1}H—^{1}H COSY (bold) and selected HMBC (arrow) correlations of pudicin.

cm^{-1}: 3350, 2908, 2873, 2850, 1715, 1647, 1614, 1566, 1454, 1376, 1342, 1308, 1239, 1214, 1123; UV λ_{max} nm (ε): 204 (680,000), 246 (1,190,000), 344 (640,000); ^{1}H and ^{13}C NMR data are shown in Table 3. The HRESI-TOF-MS of pudicin produced at m/z 600.2576 [M+Na]$^{+}$ (calculated value for $C_{30}H_{43}NO_8SNa$: m/z 600.2607) indicated the molecular formula was $C_{30}H_{43}NO_8S$. The absorption maxima of the UV spectrum were observed at 211, 248, and 342 nm. Analysis of the ^{1}H NMR (Table 4 and Fig. S4) and HSQC data (Fig. S5) revealed 4 methyls at δ_H 0.90 (H-20), 1.13 (H-19), 1.18 (H-17), and 1.50 (H-18), an acetyl group at δ_H 2.00 (H-5′), 6 methylenes at δ_H 0.89, 1.81 (H-7), 0.90, 1.76 (H-5), 1.29, 1.87 (H-4), 1.32, 1.79 (H-15), 2.90, 3.08 (H-3′), and 2.96 (H-14), 5 methyne protons at δ_H 1.46 (H-6), 1.83 (H-7a), 1.95 (H-9a), 2.39 (H-3), and 2.81 (H-12), an oxymethyne proton at 3.81 (H-16), a heteroatom bonded proton at δ_H 4.59 (H-2′), and 3 olefinic protons at δ_H 5.72 (H-8), 5.74 (H-9), 5.86 (H-11). The ^{13}C NMR (Table 4 and Fig. S6) and HSQC data showed the presence of 30 carbons classified into a ketone group at δ_C 205.2 (C-1), 2 carbonyl carbons at δ_C 173.3 (C-4′) and 173.8 (C-1′), 3 sp^2 carbons including an oxygenated carbon at δ_C 104.8 (C-1a), 137.8 (C-10a), and 183.1 (C-2), 3 sp^2 methine carbons at δ_C 117.8 (C-11), δ_C 123.5 (C-9), and δ_C 136.4 (C-8), 6 sp^3 methylene carbons at δ_C 42.7 (C-7), 41.8 (C-14), 40.1 (C-15), 37.1 (C-5), 36.0 (C-3′), and 29.1 (C-4), 3 sp^3 quaternary carbons at 79.0 (C-13), 71.2 (C-10), and 43.2 (C-2a), 7 sp^3 methyne carbons including 2 heteroatom bonded methyne carbons at δ_C 67.7 (C-16), 54.3 (C-2′), 52.3 (C-9a), 42.6 (C-3), 40.6 (C-12), 39.9 (C-7a), and 34.2 (C-6), and 5 sp^3 methyl carbons including an acetyl carbon atδ_C 25.0 (C-18), 22.9 (C-20), 22.5 (C-5′), 23.3 (C-17), and 19.3 (C-19). The gross structure of pudicin was confirmed by analyses of two-dimensional (2D) NMR data, including ^{1}H—^{1}H Correlation Spectroscopy (COSY) and Heteronuclear Multiple Bond Correlation (HMBC) spectra in CD_3OD (Fig. S7 and Fig. S8). The ^{1}H—^{1}H COSY data indicated

Table 4 ^{1}H and ^{13}C NMR chemical shifts of pudicin.

3MP-14 (CD_3OD)		
Position	δ_H	δ_C
1		205.2
1a		104.8
2		183.1
2a		43.2
3	2.39 (m,1H)	42.6
4	1.29 (m, 1H)	29.1
	1.87 (m, 1H)	
5	0.90 (overlap, 1H)	37.1
	1.76 (m, 1H)	
6	1.46 (m, 1H)	34.2
7	0.89 (overlap, 1H)	42.7
	1.81 (overlap, 1H)	
7a	1.83 (overlap, 1H)	39.9
8	5.72 (dd, J = 10.4, 10.4 Hz, 1H)	136.4
9	5.74 (dddd, J = 10.4, 10.2, 4.2, 1.8 Hz, 1H)	123.5
9a	1.95 (m, 1H)	52.3
10		71.2
10a		137.8
11	5.86 (d, J = 7.2 Hz, 1H)	117.8
12	2.81 (m, 1H)	40.6
13		79.0
14	2.96 (d, J = 7.2 Hz, 2H)	41.8
15	1.32 (overlap, 1H)	40.1
	1.79 (overlap, 1H)	
16	3.81 (q, J = 6.6 Hz, 1H)	67.7
17	1.18 (d, J = 6.6 Hz, 3H)	23.3
18	1.50 (s, 3H)	25.0
19	1.13 (s, 3H)	19.3
20	0.90 (d, J = 6.6 Hz, 3H)	22.9
1′		173.8
2′	4.59 (m, 1H)	54.3
3′	2.90 (m, 1H)	36.0
	3.08 (m, 1H)	
4′		173.3
5′	2.00 (s, 3H)	22.5

Recorded for ^{1}H NMR at 600 MHz and for ^{13}C NMR at 150 MHz in methanol-d_4 (CD_3OD).

partial structures **a** (C-3–C-6 and C3–C-7a), **b** (C-8–C-9a), **c** (C-11–C-12, C-12–C-15 and C-15–C-17), and **d** (C-2′–C-3′) as shown in Fig. 3. The partial structure **a** and the HMBC correlations from H-3 to C-7, from H-7 to C-3 and C-5, and from H-20 to C-5, C-6, and C-7 revealed methylcyclohexane frame. The partial structure **b** and the HMBC correlations from H-8 to C-3, C-7a, and C-9a, from H-9 to C-2a and C-7a, and from H-9a to C-8 revealed cyclohexene frame, confirming the connectivity of cyclohexene frame and methylcyclohexane frame at C-3 and C-7a. This bicyclic structure was also supported by the TOCSY correlations (Fig. S9). The partial structure **c** and the HMBC correlations from H-11 to C-1a and C-13, from H-12 to C-1, C-10a, and C-13, and from H-15 to C-13 revealed 5-propylcyclohex-3-en-1-one frame. The partial structure **d** and the HMBC correlations from H-2′ to C-4′, from H-3′ to C-1′, and from H-5′ to C-4′ revealed *N*-acetylcysteine moiety. The connectivity of this moiety at C-13 through C-14 was revealed by the HMBC correlations from H-3′ to C-14, from H-14 to C-3′, C-1, C-12, and C-13, and from H-12 to C-14. The HMBC correlations from H-11 to C-10, from H-11 and H-9 to C-2 (^{4}J HMBC), from H-18 to C-9a, C-10, and C-10a, from H-3 to C-19, and from H-19 to C-2, C-2a, and C-3 revealed the connectivity of 2 partial structures, 5-(2-hydroxypropyl)cyclohex-3-en-1-one frame and cyclohexene, through 4,6-dimethylcyclohex-1-en-1-ol frame. Finally, 4 hydroxy groups were attached at C-2, C-10, C-13, and C-16 by accounting for the molecular formula and chemical shifts. The central part of this structure was also supported by the data of 1D and 2D NMR measured in $CDCl_3$ (Fig. S10 to Fig. S13). As shown in Fig. S10, ^{1}H NMR showed a downfield proton signal of 2-OH (14.9 ppm). The HMBC correlations (Fig. S14) from 2-OH to C-1a, C-2, and C2a supported this structure. Thus, the planar structure was determined, as shown in Fig. 3.

Screening for antimicrobial activity

Pudicin showed no antimicrobial activity against *S. aureus* ATCC 25923, *K. rhizophila* ATCC 9341, *B. subtilis* ATCC 6633, *E. coli* ATCC 25922, *P. aeruginosa* ATCC 27853, and *C. albicans* ATCC 10231. The culture broth of strain 3MP-14 showed antibacterial activity against *S. aureus* ATCC 25923, *K. rhizophila* ATCC 9341, and *B. subtilis* ATCC 6633.

In vitro antioxidant activity of pudicin

For the DPPH assay, 500 μg/ml of pudicin showed 57.38 ± 3.88% DPPH free radical scavenging activity compared to standard ascorbic acid, which showed 89.65 ± 0.05% at 16 μg/ml concentration. The IC_{50} value of pudicin was 394.89 ± 3.88 μg/ml. For the FRAP assay, the amount of reduced iron was correlated with the antioxidant capacity of pudicin. The activity was reported in terms of ascorbic acid equivalents (μM). The 100 μg/ml of pudicin showed slight antioxidant activity as 0.02 μM of ascorbic acid equivalents.

Based on polyphasic studies, dDDH, and ANI, this strain was identified as *Streptomyces mimosae* [8, 19]. Twenty-four putative secondary metabolite BGCs were also predicted in the draft genome of strain 3MP-14 [25]. The related biosynthetic secondary metabolite genes have been emphasized as PKS type I, II, III, and NRPS. The result of PC screening suggested that strain 3MP-14 produced ikarugamycin and fumaquinone (Fig. S4). Despite no fumaquinone in the BGCs, the BGCs of ikarugamycin were detected as 12% similarity in the genome of strain 3MP-14. These data strongly support the identification of a known compound. Ikarugamycin has been reported in *Streptomyces* sp. No. 8603 [32], an endophytic

Streptomyces harbinensis NEAU-Da3^T [33], and *Streptomyces zhaozhouensis* CA-185989 [34]. It was a polycyclic tetramate macrolactam (PTMs) that exhibited antitumor, antibacterial, and antifungal activities [33–36], while fumaquinone, a prenylated naphthoquinone antibiotic, was produced by *Streptomyces fumanus* LL-F42248 and showed antimicrobial activity against Gram-positive bacteria [37].

Upon analyzing the genome of *S. mimosae* 3MP-14 and 3MP-10^T, it was discovered that the ikarugamycin BGC was present. Similarly, the genome of *S. triticirhizae* DSM 107172^T also contained the ikarugamycin BGC. Thus, by comparing the genome analyses of strains 3MP-14, 3MP-10^T, and DSM 107172^T, it can be concluded that the ikarugamycin BGCs are present in all 3 strains. This indicates that the ikarugamycin biosynthetic gene cluster is conserved within this phylogenetic cluster. As previously reported, the known piericidin A1 could be estimated from BCGs of *S. chumphonensis* KK1-2^T [38] but was absent in closely related strains unrelated to the species within the phylogenetic cluster. Therefore, combining chemical and *in silico* analysis of attractive compounds is a potential approach.

In addition to antioxidant activity, the DPPH assay of pudicin showed slight free radical scavenging activity at 50–500 μg/ml compared to ascorbic acid. Therefore, our strain could be a source of antioxidants, as reported in *Streptomyces* sp. AM-S1 [39] and a mangrove-derived *Streptomyces* sp. MUM212 [40]. Based on secondary metabolite BGC analysis, ectoine ($C_6H_{10}N_2O_2$) and naringenin ($C_{15}H_{12}O_5$) showed 100% BGC similarity; however, these secondary metabolites were not produced by strain 3MP-14 (Table 4). Nevertheless, some peaks could not be identified as known compounds in the LC chart (Fig. S4) from the PC properties and genome. Therefore, some new compounds may be left in the culture broth of strain 3MP-14. Combination of PC screening and BGC analysis could effectively search for new compounds.

CONCLUSION

Streptomyces mimosae 3MP-14 isolated from the root of *Mimosa pudica* was characterized and identified based on polyphasic approaches, the 16S rRNA gene, and genome sequence analysis. Two known compounds, ikarugamycin and fumaquinone, and a new compound, pudicin, were discovered from the culture broth of strain 3MP-14 by PC screening. Pudicin has a unique structure with a 4-membered ring and *N*-acetylcysteine moiety. It showed the presence of antioxidants in the DPPH assay. Twenty-four putative secondary metabolite BGCs were identified from the draft genome analysis of the strain.

Appendix A. Supplementary data

Supplementary data associated with this article can be found at http://dx.doi.org/10.2306/scienceasia1513-1874.2023.067.

Acknowledgements: This study was supported by the Thailand Research Fund for a 2017 Royal Golden Jubilee Ph.D. Program as a scholarship to NK, the Institute for Fermentation, Osaka (IFO), Japan, and the Grant for International Research Integration, Research Pyramid, Ratchadaphiseksomphot Endowment Fund (CUGRP_61_01_33_01), Chulalongkorn University. We thank the Pharmaceutical Research Instrument Center, Faculty of Pharmaceutical Sciences, Chulalongkorn University for providing research facilities.

REFERENCES

1. Kämpfer P (2012) Genus I. *Streptomyces* Waksman and Henrici 1943, 339AL emend. Witt and Stackebrandt 1990, 370 emend. Wellington, Stackebrandt, Sanders, Wolstrup and Jorgensen 1992, 159. In: Goodfellow M, Kämpfer P, Busse MJ, Trujillo ME, Suzuki K, Ludwig W, Whitman WB (eds) *Bergey's Manual of Systematic Bacteriology, the Actinobacteria*, Part B, 2nd edn, vol 5, Springer, New York, pp 1455–1767.
2. Takahashi Y, Nakashima T (2018) Actinomycetes, an inexhaustible source of naturally occurring antibiotics. *Antibiotics* **7**, 45.
3. Genilloud O (2017) Actinomycetes: still a source of novel antibiotics. *Nat Prod Rep* **34**, 1203–1232.
4. Matsumoto A, Takahashi Y (2017) Endophytic actinomycetes: promising source of novel bioactive compounds. *J Antibiot* **70**, 514–519.
5. Gunatilaka AL (2006) Natural products from plant-associated microorganisms: distribution, structural diversity, bioactivity, and implications of their occurrence. *J Nat Prod* **69**, 509–526.
6. Strobel G, Daisy B (2003) Bioprospecting for microbial endophytes and their natural products. *Microbiol Mol Biol Rev* **67**, 491–502.
7. Nakashima T, Takahashi Y, Ōmura S (2017) Search for new compounds from Kitasato microbial library by physicochemical screening. *Biochem Pharmacol* **134**, 42–55.
8. Klykleung N, Yuki M, Kudo T, Ohkuma M, Phongsopitanun W, Inahashi Y, Matsumoto A, Tanasupawat S (2020) *Streptomyces mimosae* sp. nov., an endophytic actinomycete isolated from the root of *Mimosa pudica* in Thailand. *Int J Syst Evol Microbiol* **70**, 3316–3322.
9. Shirling EB, Gottlieb D (1966) Methods for characterization of *Streptomyces* species. *Int J Syst Bacteriol* **16**, 313–340.
10. Kelly K (1964) *Inter-society Color Council-national Bureau of Standard Color Name Charts Illustrated with Centroid Colors*, US Government Printing Office, Washington, DC.
11. Staneck JL, Roberts GD (1974) Simplified approach to identification of aerobic actinomycetes by thin-layer chromatography. *Appl Microbiol* **28**, 226–231.
12. Minnikin DE, O'Donnell AG, Goodfellow M, Alderson G, Athalye M, Schaal A, Parlett JH (1984) An integrated procedure for the extraction of bacterial isoprenoid quinones and polar lipids. *J Microbiol Methods* **2**, 233–241.

13. Collins MD, Pirouz T, Goodfellow M, Minnikin DE (1977) Distribution of menaquinones in actinomycetes and corynebacteria. *J Gen Microbiol* **100**, 221–230.
14. Sasser M (1990) *Identification of Bacteria by Gas Chromatography of Cellular Fatty Acids*, MIDI Technical Note 101, MIDI Inc, Newark, DE.
15. Saito H, Miura K (1963) Preparation of transforming deoxyribonucleic acid by phenol treatment. *Biochem Biophys Acta* **72**, 619–629.
16. Lane DJ (1991) 16S/23S rRNA sequencing. In: Stackebrandt E, Goodfellow M (eds) *Nucleic Acid Techniques in Bacterial Systematics*, Wiley, Chichester, pp 115–148.
17. Tamura K, Stecher G, Kumar S (2021) MEGA11: molecular evolutionary genetics analysis version 11. *Mol Biol Evol* **38**, 3022–3027.
18. Bankevich A, Nurk S, Antipov D, Gurevich AA, Dvorkin M, Kulikov AS, Lesin VM, Nikolenko SI, et al (2012) SPAdes: a new genome assembly algorithm and its applications to single-cell sequencing. *J Comput Biol* **19**, 455–477.
19. Richter M, Rosselló-Móra R (2009) Shifting the genomic gold standard for the prokaryotic species definition. *Proc Natl Acad Sci USA* **106**, 19126–19131.
20. Richter M, Rosselló-Móra R, Oliver Glöckner F, Peplies J (2016) JSpeciesWS: a web server for prokaryotic species circumscription based on pairwise genome comparison. *Bioinformatics* **32**. 929–931.
21. Meier-Kolthoff JP, Auch AF, Klenk HP, Göker M (2013) Genome sequence-based species delimitation with confidence intervals and improved distance functions. *BMC Bioinformatics* **14**, 60.
22. Tatusova T, DiCuccio M, Badretdin A, Chetvernin V, Nawrocki EP, Zaslavsky L, Lomsadze A, Pruitt KD, et al (2016) NCBI prokaryotic genome annotation pipeline. *Nucleic Acids Res* **44**, 6614–6624.
23. Delcher AL, Bratke KA, Powers EC, Salzberg SL (2007) Identifying bacterial genes and endosymbiont DNA with Glimmer. *Bioinformatics* **23**, 673–679.
24. Aziz RK, Devoid S, Disz T, Edwards RA, Henry CS, Olsen GJ, Olson R, Overbeek R, et al (2012) SEED servers: high-performance access to the SEED genomes, annotations, and metabolic models. *PLOS One* **7**, e48053.
25. Blin K, Shaw S, Kloosterman AM, Charlop-Powers Z, Van Wezel GP, Medema MH, Weber T (2021) antiSMASH 6.0: improving cluster detection and comparison capabilities. *Nucleic Acids Res* **49**, W29–W35.
26. Sripreechasak P, Tanasupawat S, Matsumoto A, Inahashi Y, Suwanborirux K, Takahashi Y (2013) Identification and antimicrobial activity of actinobacteria from soils in southern Thailand. *Trop Biomed* **30**, 46–55.
27. Qin S1, Li J, Chen HH, Zhao GZ, Zhu WY, Jiang CL, Xu LH, Li WJ (2009) Isolation, diversity, and antimicrobial activity of rare actinobacteria from medicinal plants of tropical rain forests in Xishuangbanna, China. *Appl Environ Microbiol* **75**, 6176–6186.
28. Chansriniyom C, Bunwatcharaphansakun P, Eaknai W, Nalinratana N, Ratanawong A, Khongkow M, Luechapudiporn R (2018) A synergistic combination of *Phyllanthus emblica* and *Alpinia galanga* against H_2O_2-induced oxidative stress and lipid peroxidation in human ECV304 cells. *J Funct Foods* **43**, 44–54.
29. Wong CW, Cheung WS, Lau YY, Bolanos de la Torre AAS, Owusu-Apenten R (2015) A FRAP assay at pH 7 unveils extra antioxidant activity from green, black, white and rooibos tea but not apple tea. *F Nutr Report* **1**, 16–23.
30. Han C, Yu Z, Zhao J, Shi H, Hu J, Yu B, Song J, Shen Y, et al (2020) *Streptomyces triticagri* sp. nov. and *Streptomyces triticirhizae* sp. nov., two novel actinobacteria isolated from the rhizosphere soil of wheat (*Triticum aestivum* L.). *Int J Syst Evol Microbiol* **70**, 126–138.
31. Chun J, Oren A, Ventosa A, Christensen H, Arahal DR, da Costa MS, Rooney AP, Yi H, et al (2018) Proposed minimal standards for the use of genome data for the taxonomy of prokaryotes. *Int J Syst Evol Microbiol* **68**, 461–466.
32. Jomon K, Kuroda Y, Ajisaka M, Sakai H (1972) A new antibiotic, ikarugamycin. *J Antibiot* **25**, 271–280.
33. Liu C, Wang X, Zhao J, Liu Q, Wang L, Guan X, He H, Xiang W (2013) *Streptomyces harbinensis* sp. nov., an endophytic, ikarugamycin-producing actinomycete isolated from soybean root [*Glycine max* (L.) Merr]. *Int J Syst Evol Microbiol* **63**, 3579–3584.
34. Lacret R, Oves-Costales D, Gómez C, Daíz C, de la Cruz M, Pérez-Victoria I, Vicente F, Genilloud O, et al (2015) New ikarugamycin derivatives with antifungal and antibacterial properties from *Streptomyces zhaozhouensis*. *Mar Drugs* **13**, 128–140.
35. Zhang G, Zhang W, Saha S, Zhang C (2016) Recent advances in discovery, biosynthesis and genome mining of medicinally relevant polycyclic tetramate macrolactams. *Curr Top Med Chem* **16**, 1727–1739.
36. Saeed SI, Aklilu E, Mohammedsalih KM, Adekola AA, Mergani AE, Mohamad M, Kamaruzzaman NF (2021) Antibacterial activity of ikarugamycin against intracellular *Staphylococcus aureus* in bovine mammary epithelial cells *in vitro* infection model. *Biology* **10**, 958.
37. Charan RD, Schlingmann G, Bernan VS, Feng X, Carter GT (2005) Fumaquinone, a new prenylated naphthoquinone from *Streptomyces fumanus*. *J Antibiot* **58**, 271–274.
38. Phongsopitanun W, Kanchanasin P, Khanboon A, Suwanborirux K, Tanasupawat S (2021) Marine *Streptomyces chumphonensis* KK1-2^T produces piericidin A1 as the major secondary metabolite. *Science Asia* **47**, 271–276.
39. Sowndhararajan K, Kang SC (2013) Evaluation of *in vitro* free radical scavenging potential of *Streptomyces* sp. AM-S1 culture filtrate. *Saudi J Biol Sci* **20**, 227–233.
40. Tan LTH, Chan KG, Khan TM, Bukhari SI, Saokaew S, Duangjai A, Pusparajah P, Lee LH, et al (2017) *Streptomyces* sp. MUM212 as a source of antioxidants with radical scavenging and metal chelating properties. *Front Pharmacol* **8**, 276.

Appendix A. Supplementary data

Table S1 Cultural characteristics of strain 3MP-14.

Medium	Characteristic	3MP-14	3MP-10T
ISP 2	Growth	Moderate	Moderate
	Arial mycelium	Pale yellow	Pale yellow
	Substrate mycelium	Vivid yellowish green	Vivid yellowish green
	Soluble pigment	None	None
ISP 3	Growth	Moderate	Moderate
	Arial mycelium	White	White
	Substrate mycelium	Pale yellowish	Pale yellowish
	Soluble pigment	None	None
ISP 4	Growth	Good	Good
	Arial mycelium	White	White
	Substrate mycelium	Pale yellowish	Pale yellowish
	Soluble pigment	None	None
ISP 5	Growth	Poor	Poor
	Arial mycelium	Pale yellow	Pale yellow
	Substrate mycelium	Light yellow green	Light yellow green
	Soluble pigment	None	None
ISP 6	Growth	Poor	Poor
	Arial mycelium	Pale yellowish	Pale yellowish
	Substrate mycelium	yellow	Pale yellow
	Soluble pigment	None	None
ISP 7	Growth	Poor	Poor
	Arial mycelium	Pale yellow	Pale yellow
	Substrate mycelium	yellow	yellow
	Soluble pigment	None	None
NA	Growth	Good	Good
	Arial mycelium	Pale yellow	Pale yellow
	Substrate mycelium	Pale yellowish	Pale yellowish
	Soluble pigment	None	None

Table S2 Differential characteristics of strain 3MP-14 and related type strains. Strains: 1, 3MP-14; 2, *S. mimosae* 3MP-10^{T}; 3, *S. triticirhizae* DSM 107172^{T}; 4, *S. zhaozhouensis* DSM 42101^{T}; and 5, *S. sedi* JCM 16909^{T}. +, positive; w, weakly positive; −, negative. Data are from this study, except DSM 107172^{T} was from https://bacdive.dsmz.de/strain/159640 (accessed date: March 30,2023).

Characteristic	1	2	3	4	5
Enzyme activity					
Esterase (C4)	+	+	+	+	−
Leucine arylamidase	+	+	+	w	+
Valine arylamidase	+	+	+	+	+
Cystine arylamidase	w	+	+	+	w
Trypsin	+	+	+	−	−
α-Chymotrypsin	w	+	w	+	−
Alkaline phosphatase	w	w	+	−	−
Acid phosphatase	+	+	+	+	−
α-Fucosidase	+	w	+	−	−
α-Galactosidase	+	+	+	−	w
β-Galactosidase	+	+	+	−	+
α-Glucosidase	+	+	+	+	−
β-Glucosidase	+	+	+	+	−
α-Glucosaminidase	+	+	+	−	w
α-Mannosidase	+	+	+	−	w

Table S3 Cellular fatty acid compositions (%) of strain 3MP-14 and related type strains. Strains: 1, 3MP-14; 2, *S. mimosae* 3MP-10^T; 3, *S. triticirhizae* DSM 107172^T; 4, *S. zhaozhouensis* DSM 42101^T; and 5, *S. sedi* JCM 16909^T. Data are from this study, except strain DSM 107172^T [30].

Fatty acid	1	2	3	4	5
Saturated fatty acid					
$C_{16:0}$	2.0	5.8	14.2	6.7	4.3
$C_{17:0}$	2.0	–	8.1	1.2	2.2
$C_{17:0}$ cyclo	1.4	–	7.6	–	1.7
$C_{18:0}$	–	2.0	–	1.7	–
Unsaturated fatty acid					
$C_{17:1}$ ω8c	–	–	–	3.4	3.7
$C_{18:1}$ ω9c	–	–	2.4	1.8	–
Branched fatty acid					
i-$C_{10:0}$	4.5	–	–	–	–
i-$C_{14:0}$	–	1.9	–	–	–
i-$C_{15:0}$	2.6	4.1	–	–	1.3
a-$C_{15:0}$	2.8	21.8	7.3	3.1	2.4
i-$C_{16:0}$	50.8	36.2	22.0	31.6	45.9
i-$C_{17:0}$	1.7	3.5	5.2	–	1.8
i-$C_{17:0}$ 3OH	1.8	–	–	–	–
a-$C_{17:0}$	7.2	13.0	17.4	14.4	14.6
i-$C_{18:0}$	1.2	1.0	–	–	1.9
3OH-$C_{8:0}$	1.7	–	–	–	–
Unsaturated Branched					
a-$C_{15:1}$ A	–	–	–	1.2	–
i-$C_{16:1}$ G	7.7	–	–	10.0	6.1
a-$C_{17:1}$ ω9c	5.3	3.4	–	8.9	5.0
i-$C_{18:1}$ H	–	–	–	1.2	–
Summed feature 3[a]	–	–	5.1	6.6	1.8
Summed feature 5[b]	–	1.3	–	–	–
Summed feature 8[c]	–	–	0.6	1.5	–
Summed feature 9[d]	3.2	1.9	–	1.2	2.5

–, not detected. [a] $C_{16:1}$ ω7c/$C_{16:1}$ ω6c; [b] anteiso-$C_{18:0}$/$C_{18:2}$ ω6,9c; [c] $C_{18:1}$ ω7c; [d] 10Me-$C_{16:0}$. Strain DSM 107172^T contained other $C_{17:1}$ ω7c (5.6%), $C_{15:0}$ (2.2%), and $C_{18:1}$ ω8c (1.1%).

Table S4 ANIb and ANIm values (%) and the digital (*in silico*) DNA-DNA hybridization (dDDH) values between the draft genome of strain 3MP-14 and related type strains. Draft genomes: 1, Strain 3MP-14; 2, *S. mimosae* 3MP-10^T; 3, *S. triticirhizae* DSM 107172^T; 4, *S. zhaozhouensis* DSM 42101^T; and 5, *S. sedi* JCM 16909^T.

Query genome	Reference genome	ANIb	ANIm	% dDDH (Formula 2)*	Model C.I.	Distance	Prob. DDH ⩾70%	G+C difference
1	2	100	100	100	100–100%	0.0000	98.30	0.00
1	3	94.49	94.62	55.7	52.9–58.4%	0.0595	37.41	0.10
1	4	84.88	88.01	29.9	27.5–32.4%	0.1429	0.10	0.02
1	5	84.74	87.92	29.6	27.2–32.1%	0.1443	0.09	0.48

* Recommended formula (identities/HSP length), which is liberated of genome length and is thus prosperous against the use of incomplete draft genome.

Fig. S1 Polar lipid profiles of strain 3MP-14 based on two-dimensional thin layer chromatograms detected with anisaldehyde, phosphomolybdic acid, ninhydrin, Drangendorff, and Molybdenum blue as spraying reagent. Solvent system I; Chloroform:Methanol:Water (65:25:4; %, v/v). Solvent system II; Chloroform:Acetic acid:Methanol:Water (80:15:12:4; %, v/v). PE, phosphatidylethanolamine; DPG, diphosphatidylglycerol; PI, phosphatidylinositol; PG, phosphatidylglycerol; PL, unidentified phospholipid; GL, unidentified glycolipid; and PGL, unidentified phosphoglycolipid.

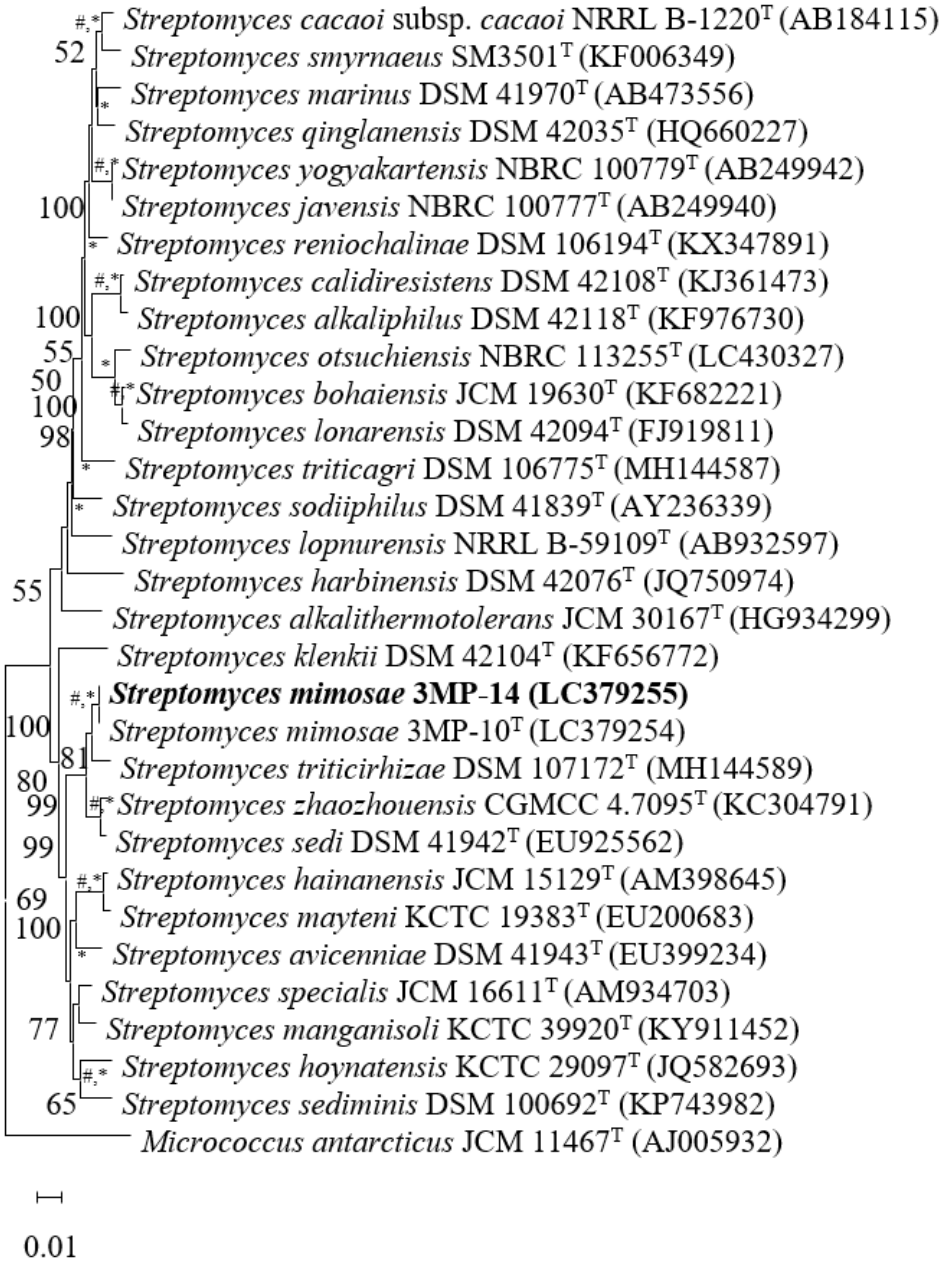

Fig. S2 Neighbor-joining phylogenetic tree based on almost complete 16S rRNA gene (1,457 nt) showing the relationship between strain 3MP-14 and *Streptomyces* species. *Micrococcus antarcticus* JCM 11467^T was used as an outgroup. The number at node showed the level of bootstrap support for branched points, based on 1000 resampling (values $\geqslant$ 50 are shown). Asterisk (*) and # indicated the branches were recovered in the maximum-likelihood and maximum-parsimony, respectively.

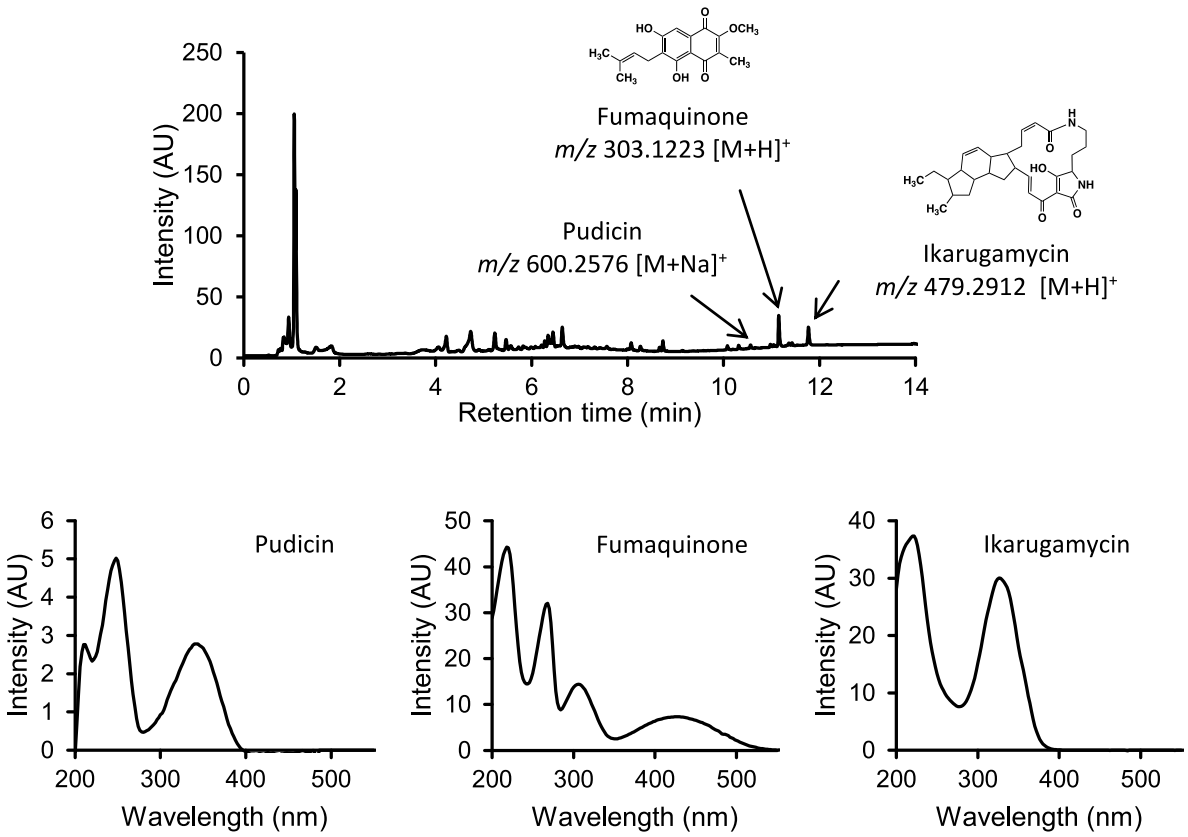

LC/MS condition in TripleTOF5600+ system

Column	Capcell Core C18 2.1φ x 100 mm (Osaka soda)
Eluate	5% MeOH in 0.1% formic acid (0 → 2 min); 5% → 100% MeOH in 0.1% formic acid (2 → 12 min); 100 % MeOH in 0.1% formic acid (12 → 14 min); detection, 254 nm.
Flow rate	0.5 mL/min
Column temp.	40℃
Detection	UV-Vis (200～600 nm), TOF-MS (*m/z* 100-2000)
Injection vol.	1 μL
Ionization mode	ESI positive
IonSpray Voltage Floating	5,500 V
Ion source gas 1	50 psi
Ion source gas 2	50 psi
Curtain gas	25 psi
Declustering Potential	80 V
temperature	500℃
Collision Energy	45 V
Collision Energy Spread	15 V
Ion Release Delay	30 μs
Ion Release Delay Width	15 μs

Fig. S3 LC-UV/MS analysis of the culture broth extracted with MeOH of strain 3MP-14.

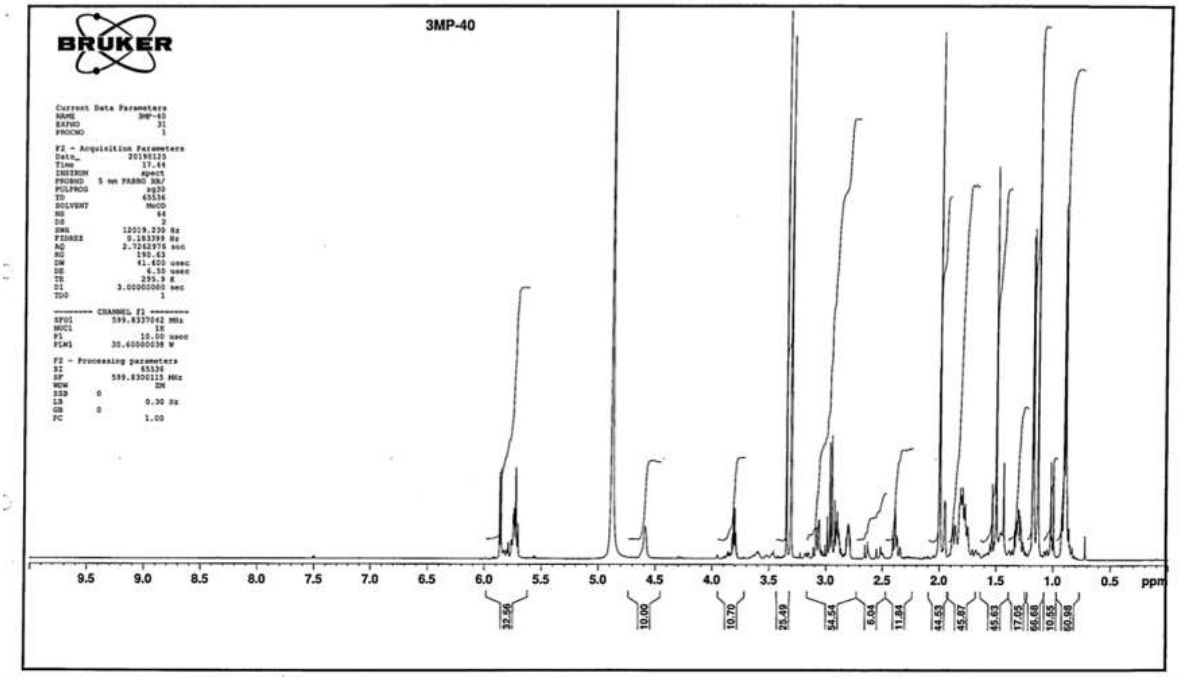

Fig. S4 ^{1}H NMR spectrum of pudicin (600 MHz, CD_3OD).

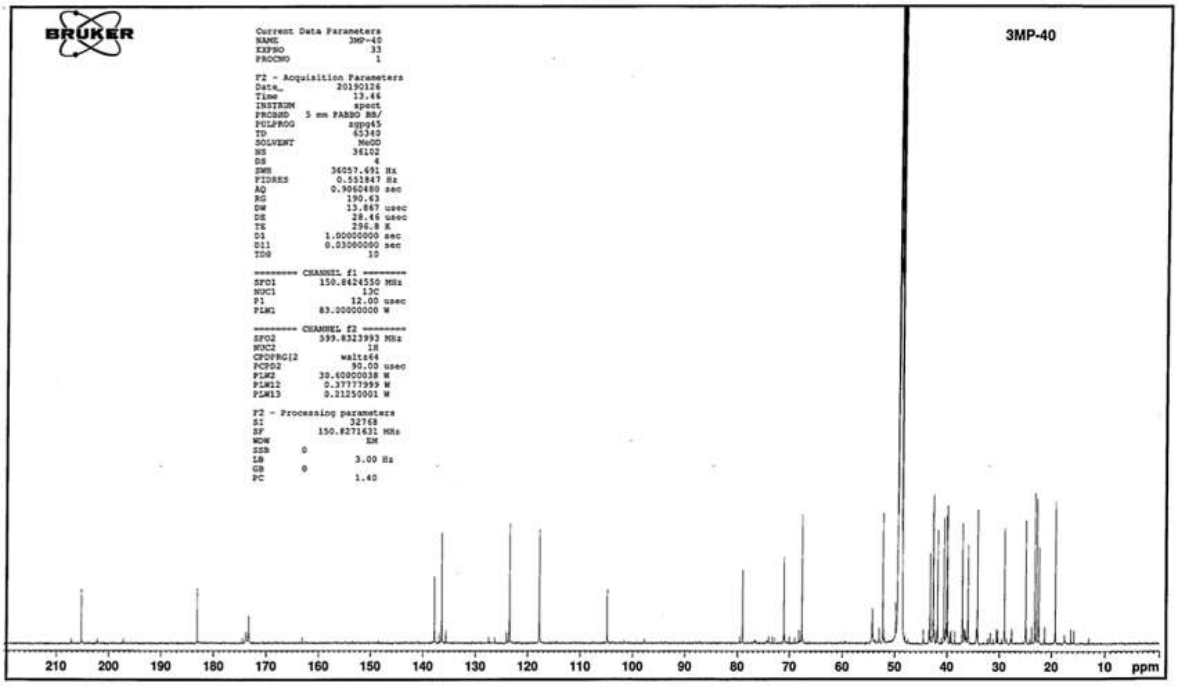

Fig. S5 ^{13}C NMR spectrum of pudicin (150 MHz, CD_3OD).

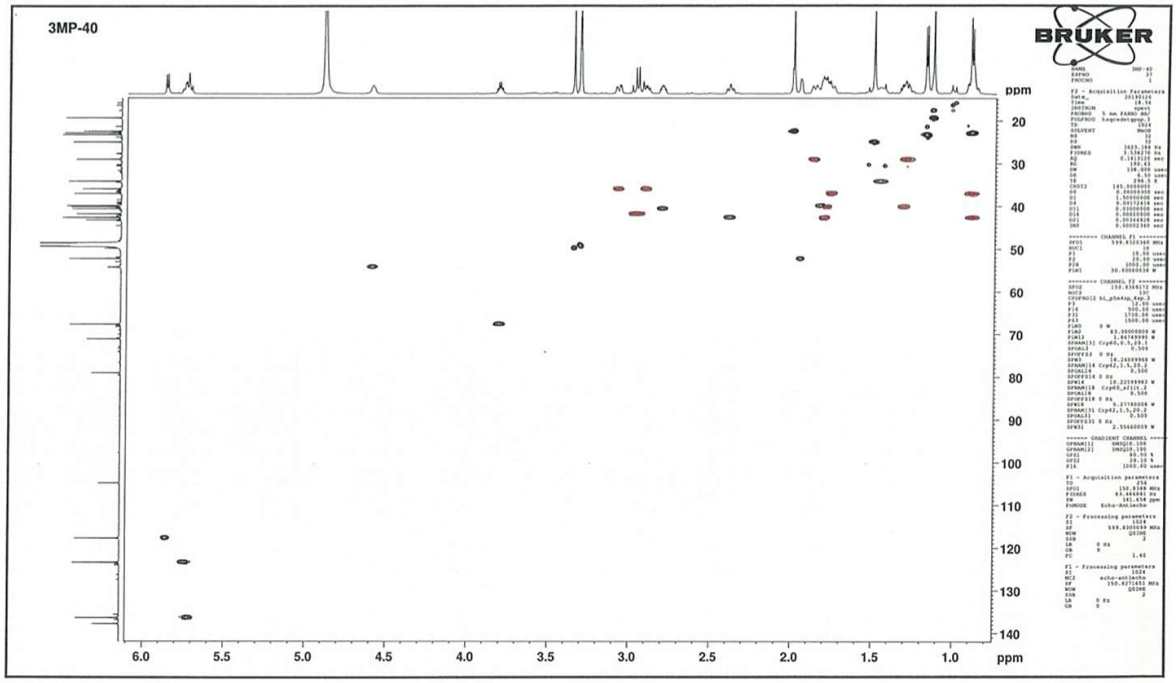

Fig. S6 HSQC spectrum of pudicin (600 MHz, CD_3OD).

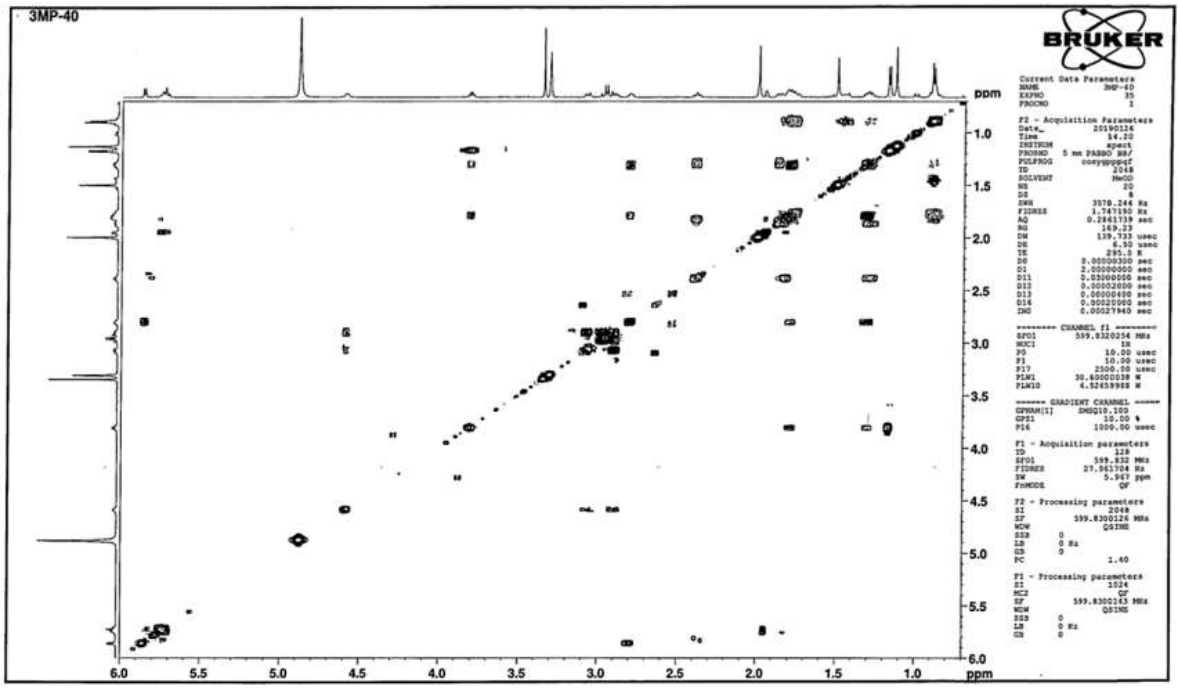

Fig. S7 ^1H—^1H COSY spectrum of pudicin (600 MHz, CD_3OD).

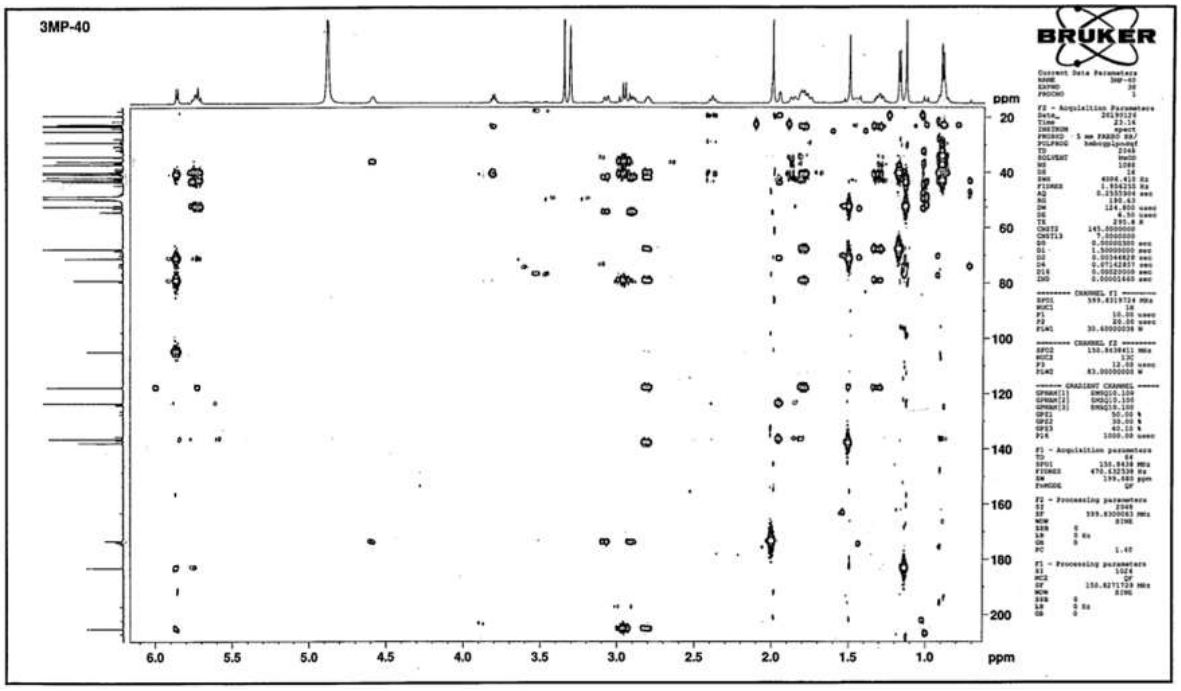

Fig. S8 HMBC spectrum of pudicin (600 MHz, CD_3OD).

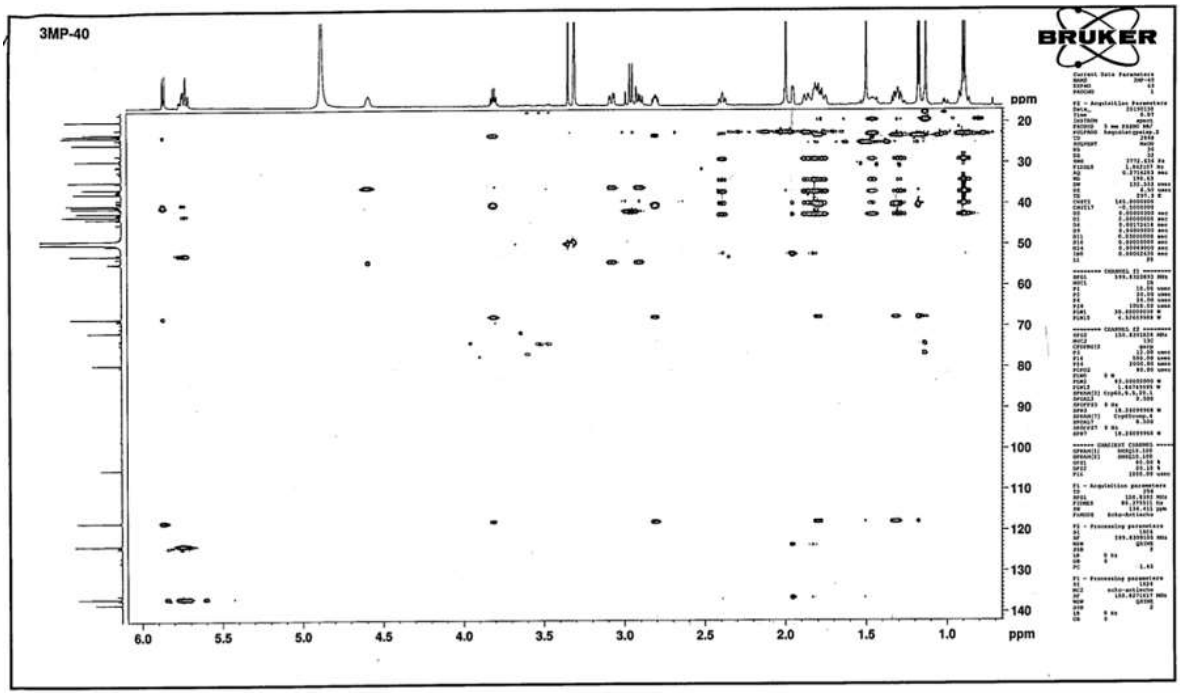

Fig. S9 TOCSY spectrum of pudicin (600 MHz, CD_3OD).

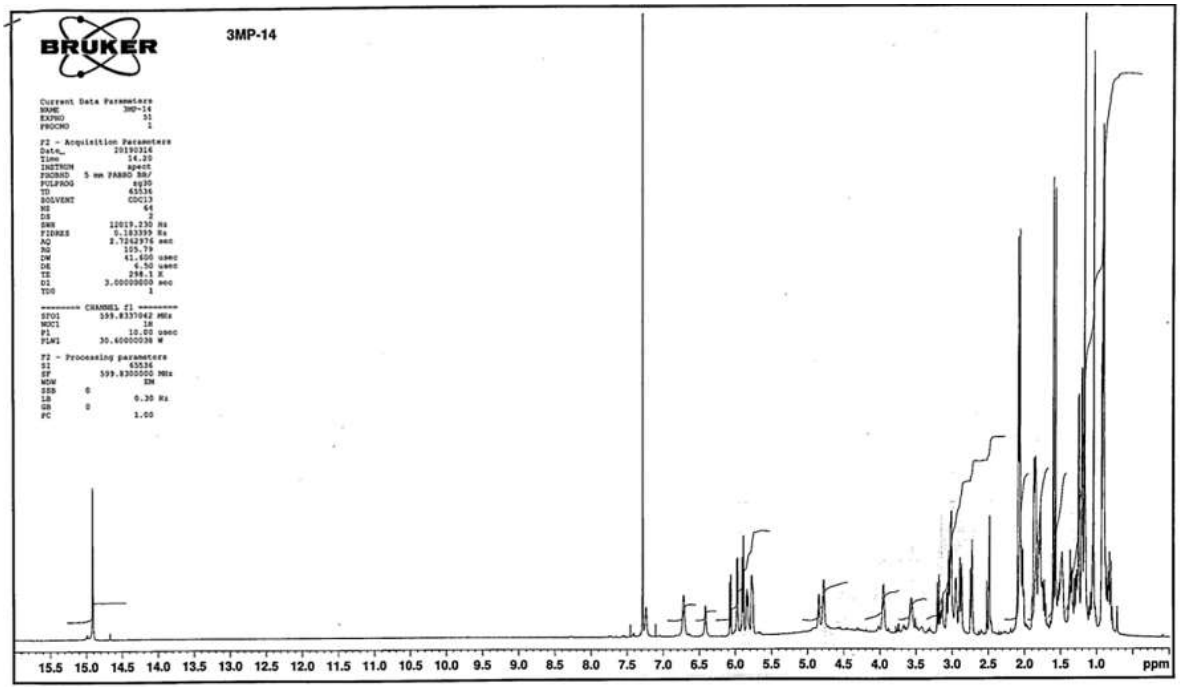

Fig. S10 ^{1}H NMR spectrum of pudicin (600 MHz, $CDCl_3$).

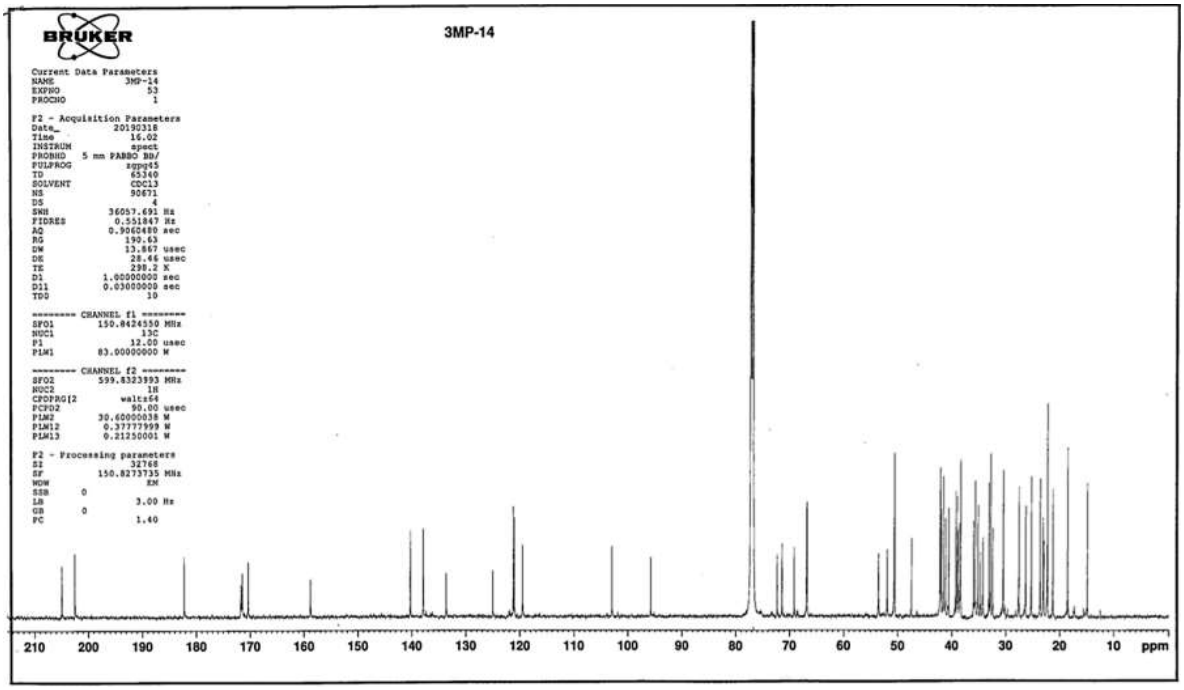

Fig. S11 ^{13}C NMR spectrum of pudicin (150 MHz, $CDCl_3$).

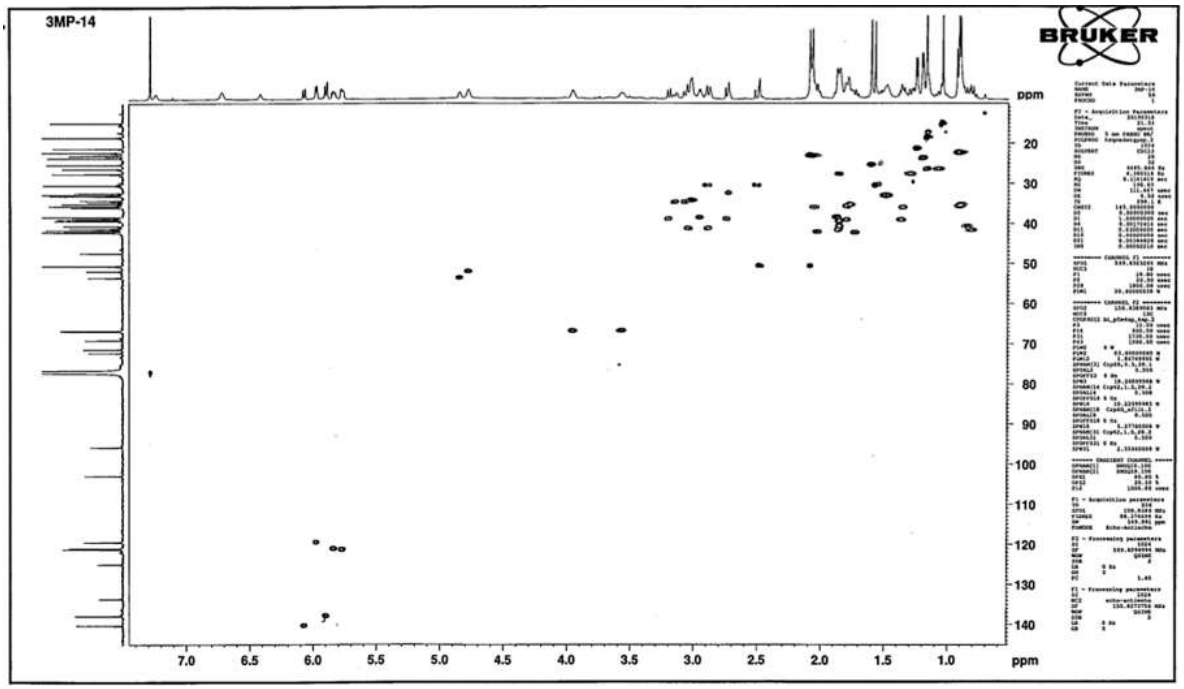

Fig. S12 HSQC spectrum of pudicin (600 MHz, $CDCl_3$).

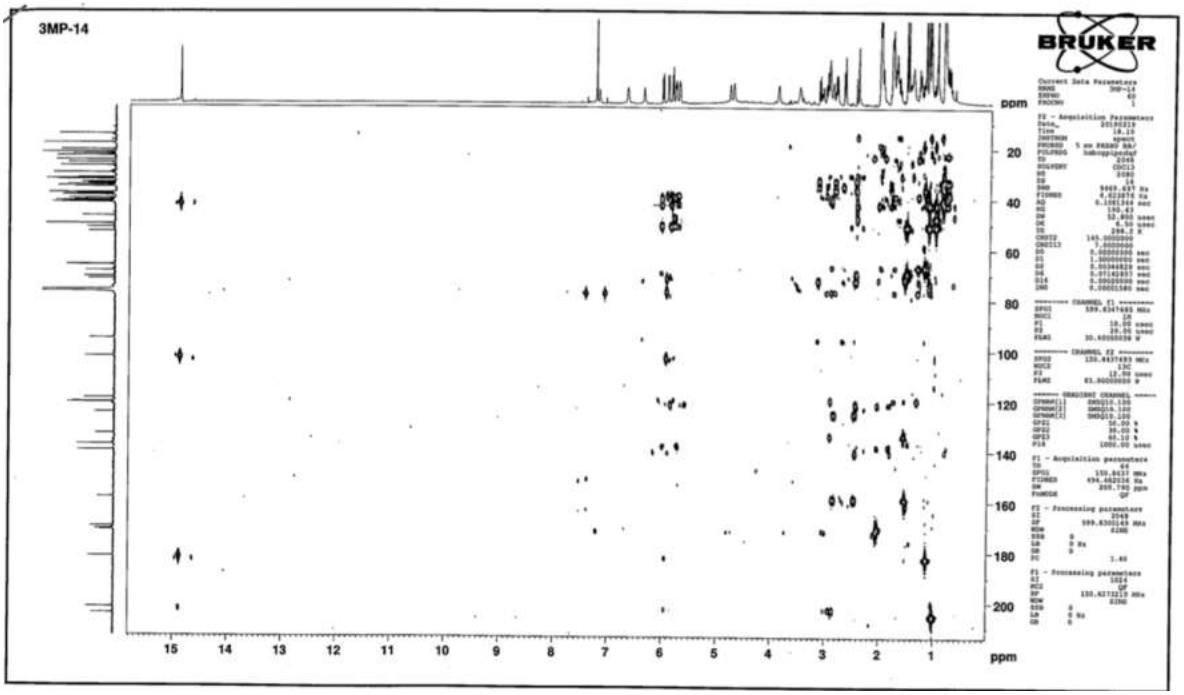

Fig. S13 HMBC spectrum of pudicin (600 MHz, $CDCl_3$).

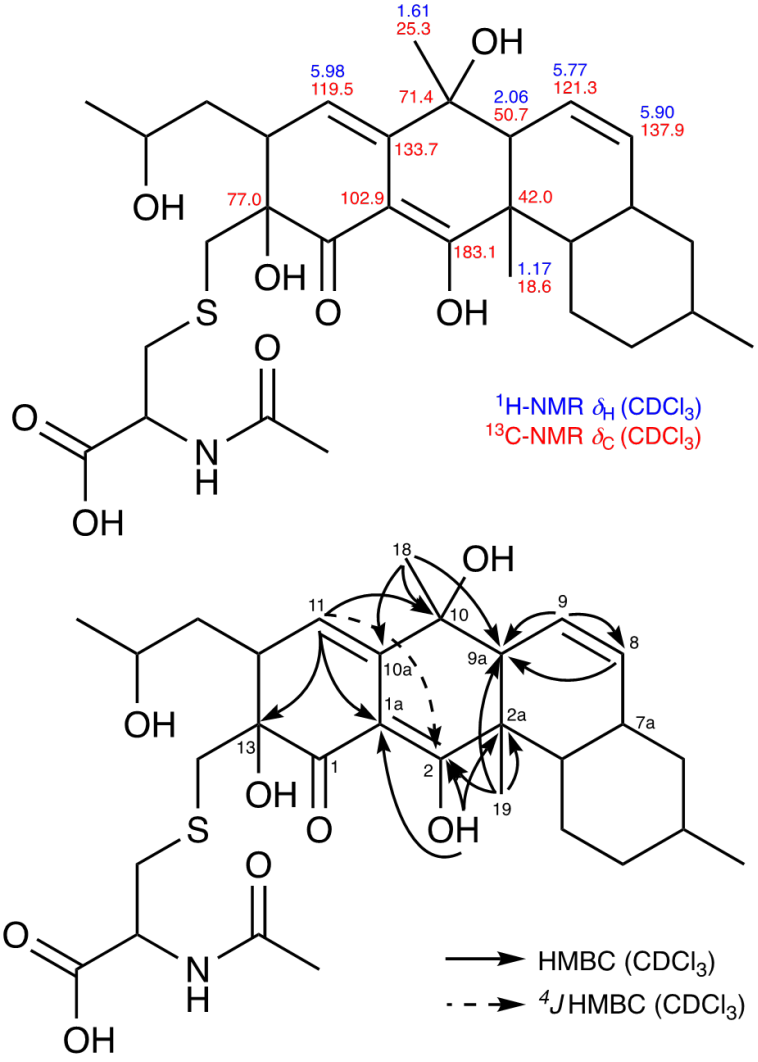

Fig. S14 Partial ^{1}H and ^{13}C NMR chemical shifts and HMBC correlations of pudicin (600 MHz, $CDCl_3$).